CrossMark

ORIGINAL PAPER

Toward a further understanding of hydrothermally pretreated holocellulose and isolated pseudo lignin

**Xiaojuan Ma · Xuefang Yang · Xin Zheng ·
Lihui Chen · Liulian Huang · Shilin Cao ·
Hannah Akinosho**

Abstract X-ray photoelectron spectroscopy (XPS) was used to trace pseudo lignin formation during the hydrothermal pretreatment of holocellulose and elaborate the structure of the isolated pseudo lignin. The results showed that XPS could detect the trace amounts of pseudo lignin in the pretreated holocellulose substrate by quantitative determination of carbon (C) and oxygen (O), while fourier transform infrared spectroscopy (FT-IR) and solid-state cross polarisation magic angle spinning carbon-13 nuclear magnetic resonance (CP/MAS ^{13}C-NMR) almost had no responses. After extensive pretreatment, C_1 increased from 8.9 to 23.0 %, O/C decreased from 0.68 to 0.54 along with an increase of Klason lignin of the pretreated holocellulose from 1.0 to 6.2 %. As for isolated pseudo lignin, both O_1 and O_2 were involved, whereas only O_1 involved in reference lignin and O_2 in holocellulose sample. In comparison to reference lignin, pseudo lignin was rich in C_1 and less in C_2, suggesting that more cyclic structures and hydroxyl groups were present in the pseudo lignin. The FT-IR and NMR results identified the presence of more aliphatic structures in the pseudo lignin, especially those formed initially; while the subsequent pretreatment could modify the aliphatic toward to aromatic structure.

Keywords XPS · Hydrothermal pretreatment · Pseudo lignin · Holocellulose

X. Ma (✉) · X. Yang · X. Zheng · L. Chen ·
L. Huang (✉) · S. Cao
College of Materials Engineering, Fujian Agriculture and Forestry University, Fuzhou 350002, China
e-mail: 1212juanjuan@163.com

L. Huang
e-mail: fafuhll@163.com

H. Akinosho
School of Chemistry and Biochemistry, Georgia Institute of Technology, Atlanta, GA 30332, USA

Introduction

X-ray photoelectron spectroscopy (XPS), also known as electron spectroscopy for chemical analysis (ESCA), is used to determine the quantitative elemental compositions, the bonding states of atoms as well as the locations of atoms in the samples (Kocaefe et al. 2013). Application of XPS to study fiber and pulp surface chemistry has been used extensively for many years, including surface composition and chemical modifications (Tóth et al. 1993; Chtourou et al. 1993; Xu et al. 2013).

In view of XPS, only peaks corresponding to C (carbon) and O (oxygen) are detected in pure cellulosic fibers; however, other elements such as N, Si, S and other metallic elements should also appear in the cellulosic fiber (Kocaefe et al. 2013; Rabemanolontsoa et al. 2011). The chemical shifts for carbon (Cls) in cellulosic fibers can be deconvoluted

into four categories C_1 (C–C/C–H), C_2 (C–O), C_3 (C=O/O–C–O) and C_4 (O–C=O) (Nzokou and Kamdem 2005; Kamdem et al. 2003). C_1 (C–C or C–H) arises mainly from lignin and extractives (Nzokou and Kamdem 2005; Johansson et al. 1999). The C1s peak centers around the bonding energy of 284 eV with a gradual decrease from C_4 to C_1. In terms of O1s peaks, O_1 (C=O) and O_2 (C–O) are generally involved; where, O_1 is primarily assigned to oxygen in lignin, while O_2 comes mainly from oxygen in carbohydrates. In fact, with an exception of C=O, C–O and C–O–C which are assigned to O_2 are also found in lignin; however, most of hydroxyls and ethers in lignin are linked to at least one benzene ring, which results in a lower bonding energy of the oxygen core level electron because of greater polarizability of the aromatic substituents. The effect leads C–O and C–O–C in lignin to the lower binding energy and thus makes them assigning to O_1 (Hua et al. 1993a). As a consequence, it is possible to monitor the amount of lignin by measuring elemental compositions and the oxygen–carbon (O/C) ratio from XPS. The O/C ratio has been shown to be proportional to the amount of C_1 (Johansson et al. 1999; Rautkari et al. 2012); O/C can be used for quantitative determination of lignin content of the substrate (Shen and Parker 1999; Zhang et al. 2014). A high O/C reflects higher cellulose and/ or hemicellulose content, while a low O/C suggests the presence of more lignin.

In our previous study from XPS, the hydrothermal pretreatment caused an increase of C_1 and a decrease in O/C for the surface substance of bamboo chips, suggesting that lignin concentrated on the surface of bamboo chips. Moreover, O/C was found to decrease to a low level that closed to lignin (Ma et al. 2013). During the hydrothermal pretreatment of holocellulose, droplets gradually formed on the surface of the holocellulose fiber (Ma et al. 2014). Studies confirmed that these spheres almost entirely composed of hydrophobic lignin, which was termed as pseudo lignin (Sannigrahi et al. 2011). In theory, the cleavage of cellulose and hemicellulose has minimal effects on its relative content of C, O and O/C; however, the pseudo lignin generated from hydrothermal pretreatment of holocellulose could result an increase of C and a corresponding decrease of O. As a result, in this study, XPS was used to trace the pseudo lignin formation and compare structural differences between pseudo lignin and reference lignin.

Experiment

Holocellulose preparation

The starting material, holocellulose, was isolated from bamboo (*Dendrocalamopsis oldhami*) chips in the lab following the acid chlorite delignification process. In brief, the bamboo chips were split into small strips and then milled through a 40-mesh screen. Afterward, the bamboo sawdust was first extracted with benzene–ethanol solution with a Soxhlet extractor followed by acid chlorite delignification process. Acetic acid and chlorite were used to delignify the bamboo sawdust; the conditions were as follows: oven-dried bamboo sawdust (500 g), liquor solid ratio 8:1, acetic acid 10 % (based on the oven-dried bamboo powder weight), chlorite 40 %, temperature 70 °C, time 60 min, and treatment times 4. The holocellulose was washed by several times until the pH close to 7. The Klason lignin content of the holocellulose was determined to be 1.0 ± 0.2 % with Tappi standard (222om-06a) without benzene–ethanol extraction (Ma et al. 2014).

Hydrothermal pretreatment

Holocellulose (150 g) was placed in a canister specially designed to fit 1000 mL stainless steel pressure vessel. After the addition of 750 mL deionized water, the pressure vessel was tightly covered with a cap and was fitted on to a shaft. Where, the shaft could rotate in a cooking apparatus that was full of thermal oil (glycerinum), the schematic diagram of the apparatus was showed and detailed described in the literature (Ma et al. 2014). The temperature of the hydrothermal reaction was controlled by the oil and was kept at 170 °C. The reaction was carried out at four time intervals (30, 90, 150 and 240 min) under constant rotation provided by the shaft. Following completion, the pressure vessel was taken out and cooled with tap water. The pretreated samples were transferred to a fine-woven nylon bag for hydrolysate liquor removal; subsequently, the residual solid was collected and washed with deionized water. The solid residue was air-dried and then vacuum dried for further analysis.

Pseudo lignin isolation from hydrothermally pretreated holocellulose

Dioxane extraction of cellulase enzymatic hydrolysis of the ball-milled powder (CEL method) was used to

isolate pseudo lignin from the pretreated holocellulose substrate (Guerra et al. 2006; Samuel et al. 2010). In brief, the vacuum-dried powder was rotary ball-milled in a porcelain jar with ceramic balls for 7 days; then, the milled powder was washed with acetic acid (HAc) and sodium acetate (NaAc) buffer (50 mmol/L, pH 4.8) and the concentration of powder-buffer mixture was kept at 20 %. Then the powder was subjected to two consecutive rounds of enzymatic hydrolysis with cellulase (*Trichoderma reesei* ATCC26921, Sigma) and cellobiase (*Aspergillus niger*, Sigma) for 2 days at 50 °C and shaken at a frequency of 150 rpm. Following centrifugation and washing the powder three times with deionized water, the powder was freeze dried. Afterward, the dried material was extracted with 96 % v/v dioxane twice at room temperature for 48 h; and then, the filtrate was recovered and concentrated. Ultimately, pseudo lignin was precipitated from the filtrate by adding water. The separate pseudo lignin was vacuum dried before the subsequent analysis. The pseudo lignin isolated from hydrothermally pretreated holocellulose was identified as PL-1 and PL-2 corresponding to the pretreatment times of 150 and 240 min, respectively. Meanwhile, the reference lignin (RL) was isolated from bamboo chips following the same procedure described above.

Acetylation of pseudo lignin and molecular weight determination

The molecular weight (MW) of the pseudo lignin was determined by GPC (gel permeation chromatography) analysis. Prior to GPC analysis, pseudo lignin was acetylated to improve its solubility in THF (tetrahydrofuran) using acetic anhydride/pyridine solutions (Samuel et al. 2010). In brief, dry pseudo lignin (100 mg) was dissolved in a 15 mL mixture of anhydride/pyridine (anhydride:pyridine = 2:1, v/v) and stirred at room temperature for 72 h in the absence of light. Thereafter, the acetylated lignin was precipitated from the mixture by adding 200 mL diethyl ether into the solution. While the acetylated lignin was freeze-dried, the samples were dissolved in the THF solution and kept the consistency of 10 mg/mL. The GPC analyses were carried out using Water GPC 2414 system consisting of three columns of Waters Styragel HR2, Waters Styragel HR3 and Waters Styragel HR4 linked in series and a refractive index (Water 2414, RI) detector. The mobile phase was THF with a flow rate

1.0 mL/min at 40 °C. The solution was filtrated with 0.45 μm membrane and injected into the GPC system for analysis, and polystyrene was used as the calibration standard. The number average molecular weight (Mn) and weight average molecular weight (Mw) were collected and processed using the Polymer Standards Service WinGPC Unity software. The polydispersity index of the molecular weight distribution was determined by calculating the ratio of Mw–Mn.

Characterizations

Solid-state cross polarisation magic angle spinning carbon-13 nuclear magnetic resonance (CP/MAS ^{13}C-NMR) measurements of the holocellulose and pretreated holocellulose (240 min pretreatment) were carried out on a Bruker Avance III 500 instrument operating at a frequency of 125.5 MHz.

Fourier transform infrared (FT-IR) spectra of the samples were obtained from Thermo Nicolet Avatar 380 FT-IR instrument; where, the samples were pelletized with KBr powder. Each spectrum was recorded in the range from 4000 to 500 cm^{-1}.

XPS (ESCAlab 250, ThermoFisher Scientific) measurements were performed on a Kratos Axis Ultra spectrometer with monochromatic Al Kα X-ray source. Both survey spectra and high-resolution spectra of C1s and O1s were collected. The atomic (C, O) composition and O/C was determined using the standard Scofield photoemission cross-sections from the XPS survey spectra; whereas the high-resolution spectra were used to differentiate and quantitate the C (C_1, C_2, C_3) and O (O_1 and O_2) by curve fitting of C1s and O1s.

The soluble state ^{1}H-NMR and ^{13}C-NMR spectra were recorded on Bruker Avance III 500 MHz spectrometer operating at a frequency of 500 and 125.5 MHz respectively. Prior to NMR analysis, the pseudo lignin samples ($\sim$70 mg) were dissolved in deuterated dimethyl sulfoxide (DMSO-d$_6$ 0.5 mL) at 50 °C via ultrasonication.

Results and discussion

Pseudo lignin formation during holocellulose hydrothermal pretreatment

As well as acid pretreatment, the hydrothermal pretreatment of holocellulose also generated pseudo

Table 1 Pseudo lignin formation during holocellulose hydrothermal pretreatment

Pretreatment time (min)	Recovery ratio (%)	Klason lignin content (%)	Yield of pseudo lignin (%)
30	79.5	1.5	Trace
90	73.3	2.0	Trace
150	71.7	3.1	58.2
240	72.3	6.2	54.1

Recovery ratio means the yield of hydrolysis, described as the ratio between the mass before and after pretreatment; yield of pseudo lignin described as the ratio between pseudo lignin (CEL method) isolated from pretreated substrate and Klason lignin content of the pretreated holocellulose

lignin, which was indicated by an increase of Klason lignin content in the pretreated holocellulose residue, as shown in Table 1. Of the small amounts of pseudo lignin formed during the hydrothermal pretreatment, only 6.2 % Klason lignin was detected in the holocellulose residue (170 °C, 240 min) and 54.1 % pseudo lignin could be isolated by CEL method. In contrast, 86.9 % of Klason lignin was present in the acid pretreated holocellulose substrate (0.20 M H_2SO_4, 60 min), while 51.3 % of the pseudo lignin was recovered by acid-dioxane extraction (Hu et al. 2012). The increase of the Klason lignin from acid pretreated residue probably suggested that acid and temperature were the main factors controlling the pseudo lignin formation. As reported by Hu, HMF (5-hydroxymethyl furfural) was the key intermediate to form pseudo-lignin (Hu and Ragauskas 2014). Moreover, cellulose degradation significantly enhanced as the temperature was elevated to 180 °C (Yan et al. 2014); more specifically, the decomposition of the sugars to HMF and F (furfural) aggravated with increasing acid concentrations (Roberto et al. 2003).

XPS characterizations of the hydrothermally pretreated holocellulose

Theoretically, C_2 (C–O) is the predominant linkage in cellulose; accordingly, the O/C of cellulose is calculated as 0.83 in light of the gross formula ($C_6H_{10}O_5$) (Hua et al. 1993a, b). In addition, O/C of hemicellulose, mainly represented by glucuronxylans, is approximately 0.8. Similar to pure cellulose, holocellulose was rich in C_2 and O_2. In principle, the O/C of holocellulose should be within the range 0.80–0.83; however, the

presence of the trace lignin decreased the O/C of holocellulose to 0.68. Another possibility that the surface might be rich in lignin than the bulk would further decrease the O/C (Johansson et al. 1999).

Surprisingly as shown in Table 2, a higher O/C and a lower C_1 has been found on the holocellulose surface when subjected to the 30 min pretreatment. The results were likely attributed to the fact that the dissolved long-chain hemicellulose fragments precipitated back onto the fiber due to the sharp decrease in solubility as the reactor was cooling (Zhang et al. 2010). After the initial pretreatment, a general increase of C_1, decrease of C_3 and O were observed. The evident increase of C_1 was accompanied with the generation of pseudo lignin. Alternatively, the continual decrease of C_3 (C=O/O–C–O) might ascribe to the decrease of the C=O/O–C–O, resulting from gradual cleavage of hemicellulose and cellulose.

The existence of C=O (C_3) in the starting holocellulose, which originated from acetyl groups in xylan, could be verified by the presence of the peak at 1730 cm^{-1} in the FT-IR spectra as shown in Fig. 1, which disappeared when the hemicellulose encountered pretreatment (Laskar et al. 2013). Unfortunately, almost no peaks related to lignin were to be found in the FT-IR spectra even though 6.2 % of lignin was involved in the pretreated holocellulose substrate. In addition, the CP/MAS NMR spectra (Fig. 2) showed that the signals at 21 and 173 ppm, which were assigned to CH_3 and C=O in acetyl group respectively, generally disappeared after holocellulose pretreatment because of the cleavage and degradation of O-acetyl in hemicellulose (Wikberg and Maunu 2004; Yelle et al. 2013). With the exception of the signals from cellulose and hemicellulose, weak signals between 140 and 160 ppm were observed and might be assigned to aromatic structure of lignin.

Pseudo lignin formation could be identified by lignin quantitation of the pretreated holocellulose; unfortunately, FT-IR and CP/MAS-NMR could not provide additional promising information because of the small amount of pseudo lignin. In spite of this, pseudo lignin formation could be observed by XPS analysis according to a sharp rise of C_1 and a decrease in O/C.

XPS characteristics of pseudo lignin

Studies have reported that pseudo lignin consisted of carbonyl, carboxylic, aromatic and aliphatic structures

Table 2 Chemical compositions of the pretreated holocellulose

C (%)	Pure cellulose[a]	Holocellulose	Pretreatment time (min)			
			30	90	150	240
C_1 (C–C, C–H)	0	8.9	7.3	12.5	17.8	23.0
C_2 (C–O)	36.0	36.1	37.1	36.2	36.5	33.2
C_3 (C=O, O–C–O)	7.3	13.8	13.7	13.2	10.5	9.2
O_2 (C–O)	56.7	39.5	41.0	38.1	35.3	34.9
O/C	0.83	0.68	0.70	0.62	0.55	0.54

[a] Hua et al. (1993b). Since holocellulose has a much higher contribution from O_2, the contribution of O_1 could be neglected
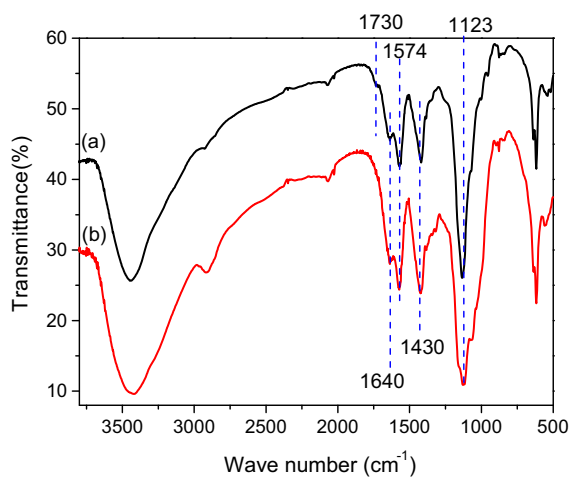
Fig. 1 FT-IR spectra of the holocellulose and pretreated holocellulose. **a** Holocellulose, **b** 240 min pretreatment
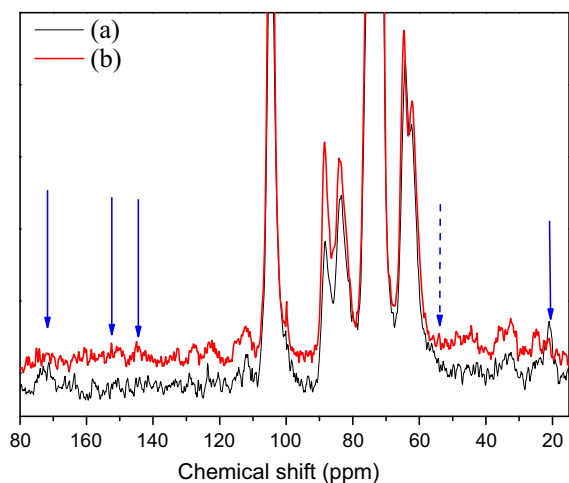

Fig. 2 CP/MAS ^{13}C-NMR spectra of the holocellulose and pretreated holocellulose. **a** Holocellulose, **b** 240 min

(Sannigrahi et al. 2011; Hu et al. 2012), however, the pseudo lignin structure has not been thoroughly investigated and remains obscure.

The high resolution scans of C1s and O1s were shown in Fig. 3a, b, whereas the deconvoluted peaks of oxygen of pseudo lignin were shown in Fig. 3c. It was apparent that C_1 represented the majority of the carbon atoms in pseudo lignin, while C_2 was the primary component of holocellulose. As for O1s scans, the bonding energy decreased from single-bonded oxygen in holocellulose to double bonded oxygen or single-bonded oxygen in reference lignin. The results further confirmed that oxygen in holocellulose came mainly from O_2, whereas O_1 are almost derived from lignin. Alternatively, both O_1 and O_2 were present in the pseudo lignin; the results might suggest that fewer hydroxyl or ethers were connected to benzene rings. As discussed earlier, the linkage between hydroxyl or ethers and benzene rings was the origin of the lower bonding energy of oxygen in hydroxyl and ethers. As shown in Table 3, pseudo lignin isolated from extensive pretreatment resulted in slightly higher O_1 and extremely lower O_2 (10.2 vs 9.8; 8.5 vs 16.0); the drastic decrease of O_2 from PL-1 to PL-2 suggested that the reactions towards pseudo lignin during hydrothermal pretreatment might take place at C–OH or C–O–C groups.

Although O/C and total C content of PL-1 was similar to the reference lignin and soda lignin (Table 3), the presence of more C_1 and less C_2 in PL-1 suggested that pseudo lignin was rich in ring structures and hydroxyl groups (C–O–H) because of the contribution to higher C_1 and lower C_2; by contrast, ether linkage (C–O–C) linkage resulted a higher C_2. It was reported that no open chain intermediates were found in xylose degradation
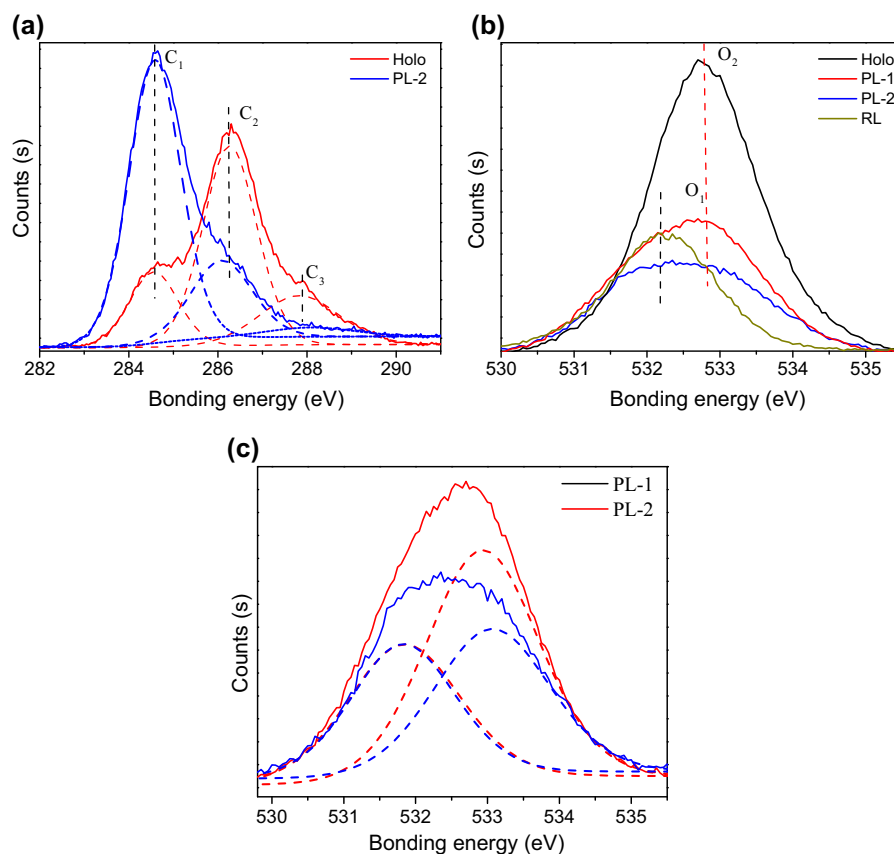
Fig. 3 High resolution scans of C1s and O1s peaks. a C1s, b O1s, c deconvoluted peaks of O1s

Table 3 Comparison of chemical compositions of the pseudo lignin and reference lignin

Sample no.	C_1 (C–C, C–H)	C_2 (C–O)	C_3 (C=O, O–C–O)	O_1	O_2	O/C
Kraft lignin[a]	39.4	28.8	5.3/2.3 (C_4)	24.2	–	0.32
Soda lignin[b]	37.5	33.5	4.0	25.9	–	0.35
Reference lignin	36.8	36.8	1.5	24.8		0.33
PL-1 (150 min)	41.9	26.9	5.4	9.8	16.0	0.35
PL-2 (240 min)	59.0	19.0	3.3	10.2	8.5	0.24

[a] Laine and Stenius (1994)
[b] Shen and Parker (1999)

products under acidic medium (Qian et al. 2005), while furfural might react with the intermediates of the xylose-to-furfural conversion and thus furfural-xylose complex might be formed (Zeitsch 2000). As a result, more alicyclic structures and C–OH (or less C–O–C) were assumed to present in the pseudo lignin.

As the pretreatment proceeded, C_1 increased alongside a decrease of C_2, C_3 and total O, suggesting that oxygen contained functional groups might participate in condensation reactions with pseudo lignin

itself or carbohydrate degradation products. The Mw and Mn of the pseudo lignin shown in Table 4 indicated repolymerization reactions; therefore aromatic rings can be alkylated significantly to produce heavy condensation compounds. The O/C of PL-2 decreased to an extremely low level and was calculated as 0.24; the low O/C value might indicate the condensed structure. Additional evidence of condensation reactions between lignin fragments also included an increase in lignin carbon–carbon bonds (Trajano

Table 4 Mw, Mn of the pseudo-lignin isolated from pretreated holocellulose

| Sample	Mw (g/mol)	Mn (g/mol)	PDI
PL-1	3.41×10^3	1.20×10^3	2.84
PL-2	5.34×10^3	3.32×10^3	1.60

et al. 2013); the results were in agreement with the C_1 content by XPS analysis.

The increase in C and decrease in O were also observed during biomass pretreatment, et al. C_9-formula calculated for the milled wood lignin (MWL) isolated from the native *Eucalyptus globulus* and pretreated substrate was $C_{900}H_{860}O_{322}(OCH_3)_{141}$ and $C_{900}H_{748}O_{283}(OCH_3)_{140}$, respectively. Following pretreatment, the O/C was reduced (Leschinsky et al. 2008a, b). Lignin residues after autohydrolysis of extractive-free aspen wood meal at 195 °C was found to be higher in carbon but lower in hydrogen and oxygen than aspen milled wood lignin (Wayman and Chua 1979). Results from a study surrounding phenolic compounds and lignin hydrothermal pretreatment showed that ether bonds were more easily broken than the C–C bonds (Barbier et al. 2012). Substantial cleavage of arylether and depletion of OCH_3 in lignin that experienced in biomass pretreatment might also be applicable in the pseudo lignin. These two effects could cause a decrease of O and O/C.

FT-IR and NMR spectra of pseudo lignin

As shown in Fig. 4a, pseudo lignin isolated from hydrothermally pretreated holocellulose shows the stretches for the O–H, C–H, C=O, aromatic C=C at 3440, 2932, 1703 and 1605/1510 cm^{-1}, respectively; which are the general structures involved in pseudo-lignin. In addition, the peak at 867 cm^{-1} arising from C–H out-of-plane bending suggests the benzene rings of pseudo-lignin are 1,3,5-trisubstituted (Hu et al. 2012). Other peaks at 1452, 1420, 1328 and 1115 cm^{-1} are likely assigned to the stretches of C=C/C–C, C–O–C, C–H of aromatic rings. More precisely, as shown in Fig. 4b, the relative intensities of the band at 1110 cm^{-1} (deformation vibrations of C–H of aromatic rings or C–O in alcohols or aliphatic ethers) to the band at 1605 and 1510 cm^{-1} (aromatic ring vibrations) were to be found in pseudo lignin rather than the reference lignin (Casas et al. 2012), which might be the structural disparities between reference lignin and pseudo lignin. Because of the weak intensity of the band at 1605 and 1510 cm^{-1}, the strong band at 1110 cm^{-1} might be assigned to the C–O in aliphatic structure; suggesting that more aliphatic hydroxyl groups and less aromatic structures appeared in pseudo lignin.

As shown in Fig. 5a, b of the ^{1}H-NMR spectra of the pseudo lignin, the signals between 6.0 and 8.0 ppm belonged to aromatic protons, whereas those between 0.8 and 1.5 ppm were assigned to the aliphatic moiety
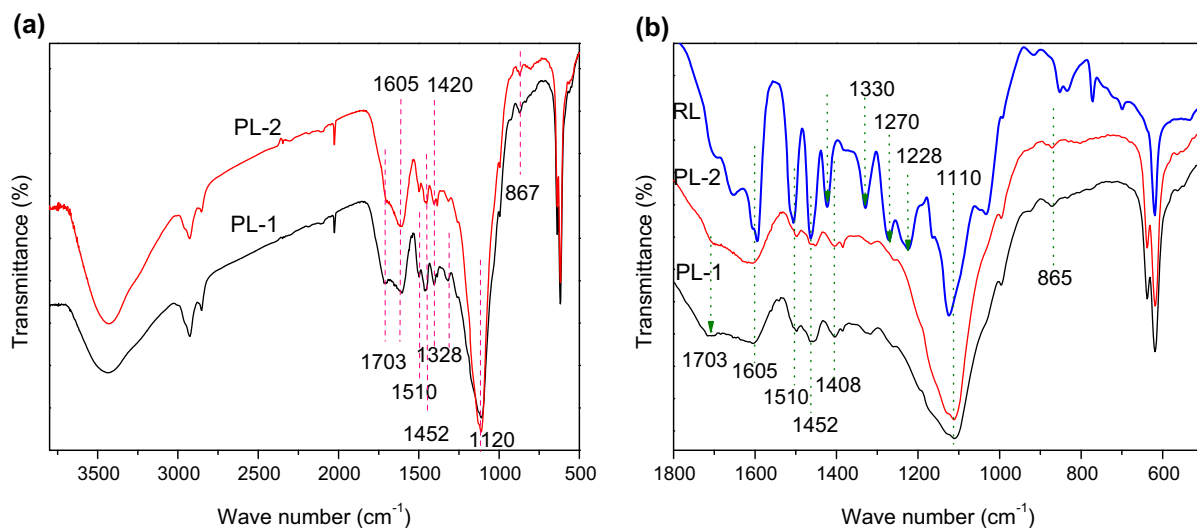
Fig. 4 FT-IR spectra of the pseudo lignin and reference lignin. **a** Pseudo lignin, **b** comparison between pseudo lignin and reference lignin (RL)
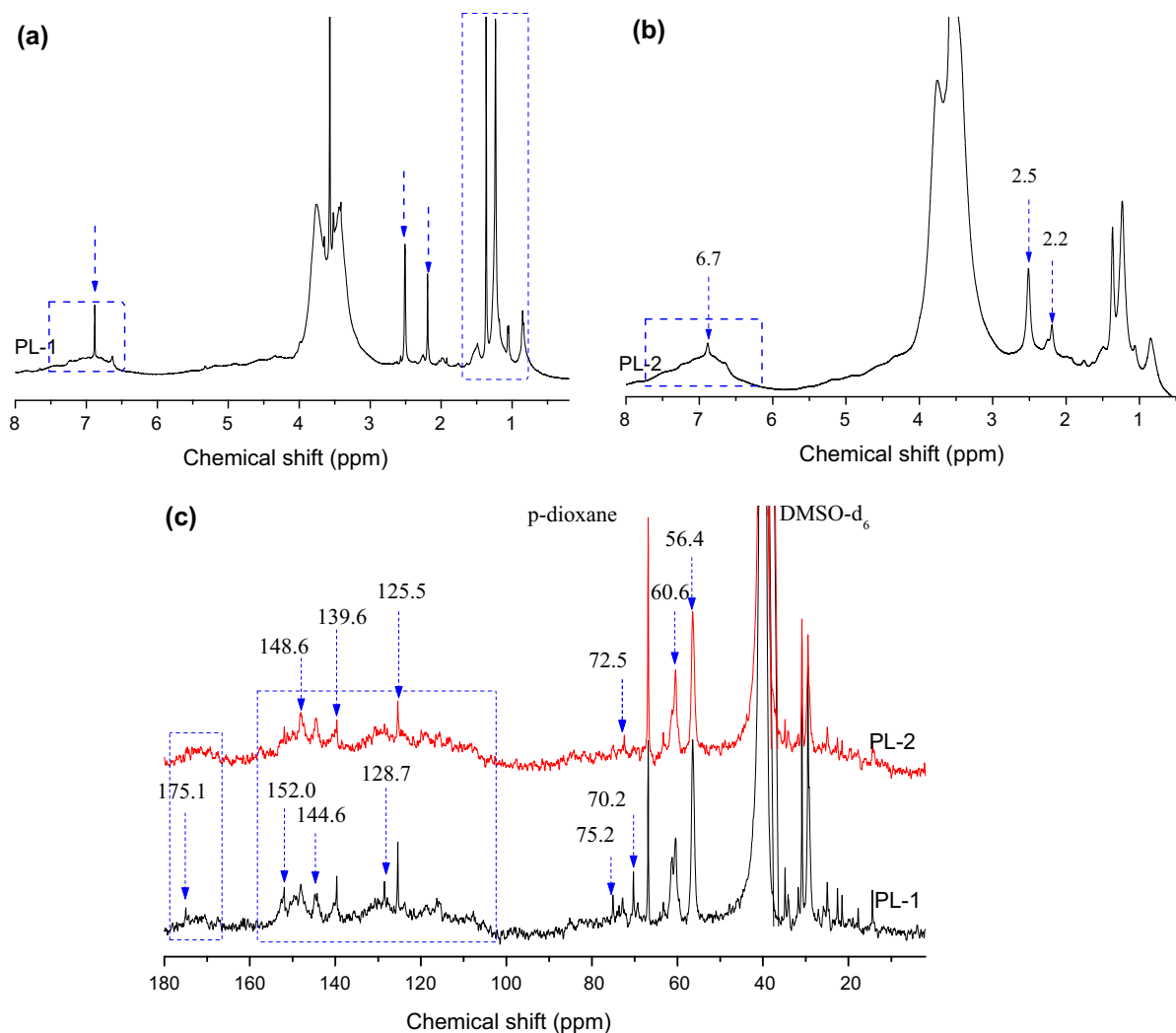
Fig. 5 ^{1}H-NMR (a, b) and ^{13}C-NMR (c) spectra of the pseudo lignin isolated from holocellulose residue

(Park et al. 1991; Tejado et al. 2007). Upon comparison with reference lignin (Fig. 6a), it was found that more aliphatic protons were present in pseudo lignin PL-1, whereas, a decrease in aliphatic protons and an increase in aromatic protons were to be found in PL-2. That was to say, the pseudo lignin formed initially might be rich in aliphatic structures. Afterward, the conversion of aliphatic to aromatic structures or the depletion of aliphatic structures might occur. In addition, the signals at 2.2 and 2.5 ppm, which might be attributed to protons in carboxylic acid or ester bond (α position) or in the acetyls connected to the benzene ring, weakened probably due to the cleavage of ester cleavage (Zoia et al. 2012; Choi and Faix 2011).

Corresponding to the ^{13}C-NMR spectra shown in Fig. 5c, the signals centered at 56.4 and 60.6 ppm were assigned to methoxyl groups connected to an aromatic ring, which were also identified by the signals between 3 and 4 ppm in ^{1}H-NMR spectrum. The origin of methoxyl group of the pseudo lignin was probably coming from 4-O-methyl-glucuronic acid in hemicellulose fractions (Hu et al. 2012; Hu and Ragauskas 2014). Besides, the comparative analysis of ^{13}C-NMR between pseudo lignin (Fig. 5c) and reference lignin (Fig. 6b), also affirmed that more aliphatic structure were involved in pseudo lignin rather than reference lignin. Accordingly, decreasing signals at 5–40 and 70–80 ppm (attributed to aliphatic structures) from
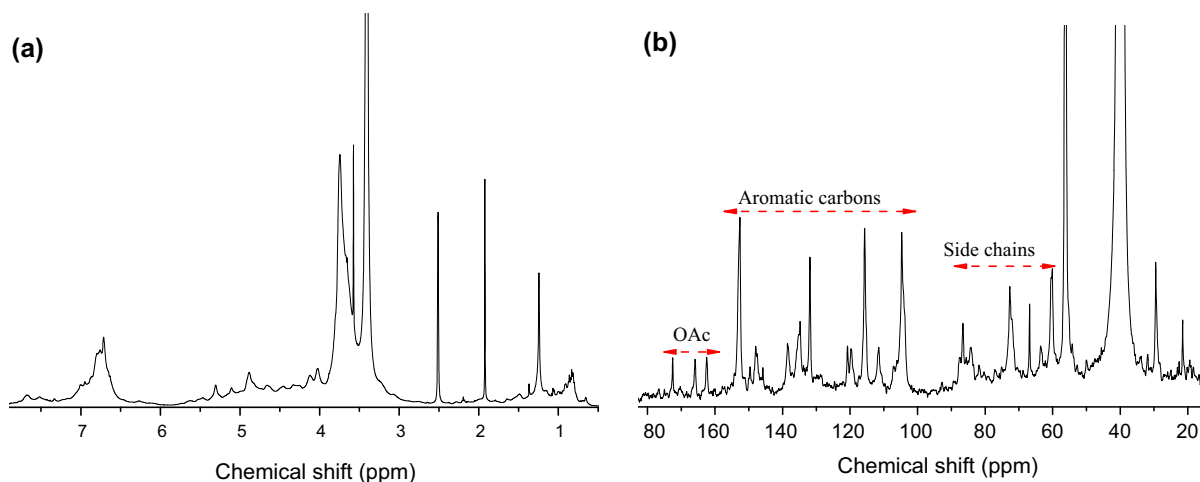
Fig. 6 ^{1}H-NMR (**a**) and ^{13}C-NMR (**b**) spectra of the reference lignin

PL-1 to PL-2 were also found in ^{13}H-NMR spectra (Kanitskaya et al. 2012), suggesting that pretreatment could convert the aliphatic structures to aromatic structure or deplete the aliphatic structure. As for the aromatic region (100–160 ppm), significant structure modifications also had been observed.

Combining the results of XPS, FT-IR and NMR, as well as Hu's study (Hu et al. 2012), pseudo lignin generated from holocellulose hydrothermal pretreatment consisted primary of carbonyl, aromatic and aliphatic structures; furthermore, more alicyclic structures and aliphatic hydroxyl groups existed in pseudo lignin. Besides, more aliphatic structures were found in pseudo lignin as opposed to reference lignin, especially for the pseudo lignin formed initially. The pretreatment modified the structure of the pseudo lignin significantly toward to an aromatic leading structure and gave rise to an increase of MW.

Conclusions

XPS, as a novel technique, can be used to determine small amounts of pseudo lignin generated in hydrothermally pretreated holocellulose by quantitative analysis of C and O atoms. During holocellulose pretreatment, C_1 increased from 8.9 to 23.0 % along with an increase in Klason lignin from 1.0 to 6.2 %. Degradation of holocellulose and subsequent reactions between degradation products caused a decrease in C_2, C_3 and O_2; however, drastic increase of C_1 led to a

lower O/C. In regards to pseudo lignin isolated from pretreated holocellulose, pseudo lignin had an extremely high content of C_1 and a low C_2 for an equivalent total C and O atoms with reference lignin; accordingly, more alicyclic structures and hydroxyl groups might be involved in pseudo lignin. Moreover, the pseudo lignin formed initially was rich in aliphatic structures, and the pretreatment might convert or deplete the aliphatic structures, and therefore pseudo lignin was toward to aromatic leading compounds.

References

Barbier J, Charon N, Dupassieux N, Serani AL, Mahé L, Ponthus J, Courtiade M, Ducrozet A, Quoineaud A, Cansell F (2012) Hydrothermal conversion of lignin compounds. A detailed study of fragmentation and condensation reaction pathways. Biomass Bioenergy 46:479–491

Casas A, Alonso MV, Oliet M, Rojo E, Rodríguez F (2012) FTIR analysis of lignin regenerated from *Pinus radiata* and *Eucalyptus globulus* woods dissolved in imidazolium-based ionic liquids. J Chem Technol Biotechnol 87:472–480

Choi JW, Faix O (2011) NMR study on residual lignins isolated from chemical pulps of beech wood by enzymatic hydrolysis. J Ind Eng Chem 17:25–28

Chtourou H, Riedl B, Kokta BV (1993) ESCA and FTIR study of synthetic pulp fiber modified by fluorinated gases and corona discharge. J Colloid Interface Sci 158:96–104

Guerra A, Filpponen I, Lucia LA, Argyropoulos DS (2006) Comparative evaluation of three lignin isolation protocols for various wood species. J Agric Food Chem 54:9696–9705

Hu F, Ragauskas A (2014) Suppression of pseudo-lignin formation under dilute acid pretreatment conditions. RSC Adv 4(9):4317–4323

Hu F, Jung S, Ragauskas A (2012) Pseudo-lignin formation and its impact on enzymatic hydrolysis. Bioresour Technol 117:7–12

Hua X, Kaliaguine S, Kokta BV, Adnot A (1993a) Surface analysis of explosion pulps by ESCA. 2. Oxygen (1s) and sulfur (2p) spectra. Wood Sci Technol 28(1):1–8

Hua X, Kaliaguine S, Kokta BV, Adnot A (1993b) Surface analysis of explosion pulps by ESCA.1. Carbon (1s) spectra and oxygen-to-carbon ratios. Wood Sci Technol 27(6):449–459

Johansson LS, Campbell JM, Koljonen K, Stenius P (1999) Evaluation of surface lignin on cellulose fibers with XPS. Appl Surf Sci 144–145:92–95

Kamdem DP, Roedl B, Adnot A, Kaliaguine S (2003) ESCA spectroscopy of poly(methyl methacrylate) grafted onto wood fibers. J Appl Polym Sci 43:1901–1912

Kanitskaya LV, Gogotov AF, Khai DTT, Rokhin AV (2012) Quantitative ^{13}C NMR spectroscopy. Chemical structure of kraft and nitrosatedlignins. Russ J Bioorg Chem 38(7):720–725

Kocaefe D, Huang X, Kocaefe Y, Boluk Y (2013) Quantitative characterization of chemical degradation of heat-treated wood surfaces during artificial weathering using XPS. Surf Interface Anal 45:639–649

Laine J, Stenius P (1994) Surface characterization of unbleached kraft pulps by means of ESCA. Cellulose 1:145–160

Laskar DD, Zeng J, Yan L, Chen S, Yang B (2013) Characterization of lignin derived from water-only flowthrough pretreatment of Miscanthus. Ind Crops Prod 50:391–399

Leschinsky M, Zuckerstätter G, Weber HK, Patt R, Sixta H (2008a) Effect of autohydrolysis of Eucalyptus globulus wood on lignin structure. Part 2: influence of autohydrolysis intensity. Holzforschung 62:653–658

Leschinsky M, Zuckerstätter G, Weber HK, Patt R, Sixta H (2008b) Effect of autohydrolysis of Eucalyptus globulus wood on lignin structure. Part 1: comparison of different lignin fractions formed during water prehydrolysis. Holzforschung 62:645–652

Ma XJ, Cao SL, Lin L, Luo XL, Chen LH, Huang LL (2013) Surface characterizations of bamboo substrates treated by hot water extraction. Bioresour Technol 136:757–760

Ma XJ, Cao SL, Chen LH, Huang LL (2014) Lignin removal and benzene–alcohol extraction effects on lignin measurements of the hydrothermal pretreated bamboo substrate. Bioresour Technol 151:244–248

Nzokou P, Kamdem DP (2005) X-ray photoelectron spectroscopy study of red oak—(Quercus rubra), black cherry—(Prunus serotina) and red pine—(Pinus resinosa) extracted wood surfaces. Surf Interface Anal 37:689–694

Park JS, Enoki M, Ohbu A, Fan K, Niki K, Akutsu H (1991) Properties of aromatic residues in ferricytochrome c$_3$ of desulfovibrio vulgaris Miyazaki f studied by ^{1}H NMR. J Mol Struct 242:343–353

Qian X, Nimlos MR, Johnson DK, Himmel ME (2005) Acidic sugar degradation pathways. Appl Biochem Biotechnol 121–124:989–997

Rabemanolontsoa H, Ayada S, Saka S (2011) Quantitative method applicable for various biomass species to determine their chemical composition. Biomass Bioenergy 35:4630–4635

Rautkari L, Hänninen T, Johansson LS, Hughes M (2012) A study by X-ray photoelectron spectroscopy (XPS) of the chemistry of the surface of Scots pine (Pinus sylvestris L.) modified by friction. Holzforschung 66:93–96

Roberto IC, Mussatto SI, Rodrigues RCLB (2003) Dilute-acid hydrolysis for optimization of xylose recovery from rice straw in a semi-pilot reactor. Ind Crops Prod 17(3):171–176

Samuel R, Pu Y, Raman B, Ragauskas AJ (2010) Structural characterization and comparison of switchgrass ball-milled lignin before and after dilute acid pretreatment. Appl Biochem Biotechnol 162:62–74

Sannigrahi P, Kim DH, Jung S, Ragauskas A (2011) Pseudo-lignin and pretreatment chemistry. Energy Environ Sci 4:1306–1310

Shen W, Parker IH (1999) Surface composition and surface energetics of various eucalypt pulps. Cellulose 6(1):41–55

Tejado A, Peña C, Labidi J, Echeverria JM, Mondragon I (2007) Physico-chemical characterization of lignins from different sources for use in phenol–formaldehyde resin synthesis. Bioresour Technol 98:1655–1663

Tóth A, Faix O, Rachor G, Bertóti I, Székely T (1993) ESCA (XPS) study on light-induced yellowing of thermomechanical and chemothermomechanical pulps. Appl Surf Sci 72:209–213

Trajano HL, Engle NL, Foston M, Ragauskas AJ, Tschaplinski TJ, Wyman CE (2013) The fate of lignin during hydrothermal pretreatment. Biotechnol Biofuels 6:110

Wayman M, Chua MGS (1979) Characterization of autohydrolysis aspen (Populus tremuloides) lignins. 4. Residual autohydrolysis lignin. Can J Chem 57(19):2612–2616

Wikberg H, Maunu SL (2004) Characterisation of thermally modified hard—and softwoodsby ^{13}C CPMAS NMR. Carbohydr Polym 58:461–466

Xu G, Wang Li, Liu J, Wu J (2013) FTIR and XPS analysis of the changes in bamboo chemical structure decayed by white-rot and brown-rot fungi. Appl Surf Sci 280:799–805

Yan L, Greenwood AA, Hossain A, Yang B (2014) A comprehensive mechanistic kinetic model for dilute acid hydrolysis of switchgrass cellulose to glucose, 5-HMF and levulinic acid. RSC Adv 4(45):23492–23504

Yelle DJ, Kaparaju P, Hunt CG, Hirth K, Kim H, Ralph J, Felby C (2013) Two-dimensional nmr evidence for cleavage of lignin and xylan substituents in wheat straw through hydrothermal pretreatment and enzymatic hydrolysis. Bioenergy Res 6:11–221

Zeitsch K (2000) The chemistry and technology of furfural and its many byproducts. Elsevier, Amsterdam

Zhang DF, Montañés F, Srinivas K, Fornari T, Ibáñez E, King JW (2010) Measurement and correlation of the solubility of carbohydrates in subcritical water. Ind Eng Chem Res 49:6691–6698

Zhang J, Zhang H, Zhang J (2014) Evaluation of liquid ammonia treatment on surface characteristics of hemp fiber. Cellulose 21:569–579

Zoia L, Tolppa EL, Pirovano L, Salanti A, Orlandi M (2012) ^{1}H-NMR and ^{31}P-NMR characterization of the lipidfraction in archaeological ointments. Archaeometry 54(6):1076–1099